Reexamination of Shear Lag in HSS Tension Members with Side Gusset Plate Connections

AKASHDEEP A. BHAT and PATRICK J. FORTNEY
In memory of Patrick J. Fortney, who passed away in October, 2019.

ABSTRACT

This paper presents an evaluation of the shear lag factor for HSS tension members connected with two side plate gussets with longitudinal welds as given in AISC *Specification* Table D3.1, Case 6b. The current AISC *Specification* for Case 6b does not permit weld lengths less than the perpendicular distance between the welds and has the potential of producing negative shear lag factors. Similar issues previously existed for members given in Case 4 of Table D3.1. However, the AISC *Specification* has adopted a mathematical model proposed by Fortney and Thornton for Case 4 of Table D3.1. The work presented in this paper (1) offers a mathematical model for calculating the shear lag factor for Case 6b derived by repurposing the model adopted by AISC for Case 4 of Table D3.1, (2) offers the results of a parametric study comparing the results of the new mathematical model to the results using the current AISC method, and (3) discusses the protocols developed for use in finite element analysis to evaluate the effectiveness of the proposed mathematical model. The proposed new mathematical model will permit longitudinal weld lengths less than the perpendicular distance between the welds and removes the possibility of calculating a negative shear lag factor, while better representing the redistribution of cross-sectional stress near the connection region.

Keywords: Shear lag, HSS, longitudinal welds, gusset plates.

BACKGROUND

The performance of a tension member is influenced by factors like size, material, type of connection, and the like. The manner in which the tension member is connected has a direct influence on shear lag. Tension members are generally connected to elements such as gusset plates using bolts or welds. When some, but not all the elements of the cross section of a tension member (e.g., flange, web, leg, etc.) are used to transfer the axial load to the connection, a nonuniform stress distribution occurs in the tension member adjacent to the connection, this phenomenon is commonly referred to as shear lag (Fortney and Thornton, 2012). Due to this effect, the entire cross section is not fully effective to carry the load at the critical section, resulting in reduced design strength of the member.

In an HSS tension member connected with two side gusset plates on opposite faces, the longitudinal welds receive the load from the gusset plate through shear. The shear in the welds is then transferred to the HSS section as an axial load. The transition from this localized stress to a uniformly distributed stress over the tension member cross section away from the connected region is a region thought to be subjected to the shear lag phenomenon. Along this critical length of the tension member, this shear lag effect can have a detrimental effect on the tensile capacity of the tension member.

Generally, the reduced capacity of a tension member is addressed through the use of a shear lag factor, U_A, applied to the gross area of the tension member. AISC *Specification for Structural Steel Buildings* (AISC, 2016), Table D3.1, requires an accounting for shear lag for various types of end connections. For HSS members connected with two side gusset plates with longitudinal welds (of length l), and considering the perpendicular distance between the welds as H, the shear lag factor is calculated using Case 6b of Table D3.1 as shown in Table 1.

INTRODUCTION

The current AISC *Specification* procedure for determining the shear lag factor for Case 6b assumes that the welds will transfer the entire member load to the two walls parallel with the gusset plates and assumes the walls that are perpendicular to the gusset plates are unconnected elements. An additional assumption made for the current Case 6b is that the perpendicular distance between the welds is equal to the width of the H side (which is parallel to the gusset plate). However, the authors propose that all four walls are connected by the welds, and as such, the perpendicular distance between the welds could be taken as either H or B, depending on which sides of the HSS the gusset plates are attached to. With this, one could argue that the eccentricity, $\bar{x}$, could

Patrick J. Fortney, Associate Professor, University of Cincinnati, Cincinnati, Ohio. In memory of Patrick J. Fortney, who passed away in October, 2019.

Akashdeep Bhat, Graduate Student, University of Cincinnati, Cincinnati, Ohio. Email:bhataa@mail.ic.edu (corresponding)

Paper No. 2019-06

Table 1. Shear Lag Factor Case 6b				
Case	Description of Element		Shear Lag Factor, UA	Example
6	Rectangular HSS	With two side gusset plates	$l \geq H ... U_A = 1 - \frac{\bar{x}}{l}$ $\bar{x} = \frac{B^2}{4(B+H)}$	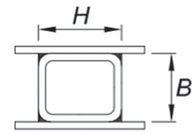

Table 2. Connection Eccentricity $\bar{x}$	
Perpendicular Distance between Welds	$\bar{x}$
H	$\bar{x} = \frac{B^2}{4(B+H)}$
B	$\bar{x} = \frac{H^2}{4(B+H)}$

be calculated in two different ways (as shown in Table 2) for a rectangular HSS, giving two possible shear lag factors.

Furthermore, the current AISC *Specification* Case 6b does not permit weld lengths less than the perpendicular distance between the welds. When the length of the connection, l, is less than the connection eccentricity, $\bar{x}$, and the gusset plates are attached to the B side, the equation produces a negative shear lag factor. For example, for an HSS 20×4×½ with the gusset plate attached to the B side (4-in. side) with welds of length l = 4 in., the connection eccentricity and the shear lag factor, using the current AISC *Specification* Case 6b, can be calculated as:

$$\bar{x} = \frac{H^2}{4(B+H)}$$
$$= \frac{(20 \text{ in.})^2}{4(20 \text{ in.} + 4 \text{ in.})}$$
$$= 4.17 \text{ in.}$$
$$U_A = 1 - \frac{\bar{x}}{l}$$
$$= 1 - \frac{4.17 \text{ in.}}{4 \text{ in.}}$$
$$= -0.04$$

This is problematic because any connection, even one with a relatively short connection length, will provide some level of force transfer.

To overcome these shortcomings, a mathematical model was developed by repurposing the mathematical model developed by Fortney and Thornton (2012) in AISC *Specification* Table D3.1, Case 4 (AISC, 2016). Subsequent to the development of the mathematical model, a parametric study was performed comparing the shear lag factor calculated using the current AISC *Specification* to that calculated using the proposed new mathematical model. A series of finite element models were then developed in ABAQUS (2013) to evaluate the validity of the mathematical model. For the new model proposed, the welds are considered to connect all four of the HSS walls, and the weld length need not necessarily be equal to or greater than the perpendicular distance between the welds. The following presents the new proposed model.

MATHEMATICAL MODEL

Fortney and Thornton (2012) proposed a new method for evaluating the shear lag factor for Case 4 as given in Table D3.1 of the 2010 AISC *Specification* (AISC, 2010) addressing the longitudinally welded end-connected members in a more general way. The objective of that work was to develop a generalized procedure for calculating shear lag in plates, angles, channels, and tee members connected with longitudinal welds. Consideration was given to connections with weld lengths less than the perpendicular distance between the welds and also to address the condition where connections have unequal weld lengths. Fortney and Thornton compared three models for evaluating the shear lag factor: (1) the AISC model (prior to 2016), (2) the Canadian Standards Association (CSA) model, and (3) a fixed-fixed beam model.

The fixed-fixed beam model proposed by Fortney and Thornton captures the biplanar shear lag effect due to the connected and unconnected elements of a section. At the time of that study, the current AISC *Specifications* considered only uniplanar shear lag effects. The recommendation proposed by Fortney and Thornton was adopted by the AISC *Specification* for Case 4 of Table D.3.1 with the by-product effect that certain shapes moved from Case 2 to Case 4. Based on the generalized biplanar model proposed, a similar approach may be taken that will address issues with Case 6b of Table D3.1 for HSS tension members connected with two side gusset plates.

It is postulated that the longitudinal welds connect all four walls of the HSS and each wall acts similarly to plates with longitudinal welds (similar to plates as shown for Case 4 in Table D3.1). Thus, only in-plane shear lag exists, eliminating the connection eccentricity ($\bar{x} = 0$). Figure 1 shows the migration of the load in the HSS walls to the four weld lines. As can be seen in the Figure 1, each weld line attracts load from both walls connected by the weld.

The total tension load carried by each wall is proportional to the relative areas of each of the four HSS walls as given by Equations 1 and 2.

$$P_B = P_u\left(\frac{B}{B+H}\right) \tag{1}$$

$$P_H = P_u\left(\frac{H}{B+H}\right) \tag{2}$$

Note that the shear lag factor will be different for the B and H walls since the l/w ratio can be different for B and H.

The generalized shear lag factor given for Case 4 is:

$$U = \frac{3l^2}{3l^2 + w^2}\left(1 - \frac{\bar{x}}{l}\right) \tag{3}$$

The shear lag factor for the B walls is given by:

$$\begin{aligned} U_B &= \frac{1}{1+\frac{1}{3}\left(\frac{w}{l_w}\right)^2}\left(1-\frac{\bar{x}}{l_w}\right) \\ &= \frac{1}{1+\frac{1}{3}\left(\frac{B}{l_w}\right)^2}\left(1-\frac{0}{l_w}\right) \\ &= \frac{3l_w^2}{3l_w^2 + B^2} \end{aligned} \tag{4}$$

The shear lag factor for the H walls is given by:

$$\begin{aligned} U_H &= \frac{1}{1+\frac{1}{3}\left(\frac{w}{l_w}\right)^2}\left(1-\frac{\bar{x}}{l_w}\right) \\ &= \frac{1}{1+\frac{1}{3}\left(\frac{H}{l_w}\right)^2}\left(1-\frac{0}{l_w}\right) \\ &= \frac{3l_w^2}{3l_w^2 + H^2} \end{aligned} \tag{5}$$

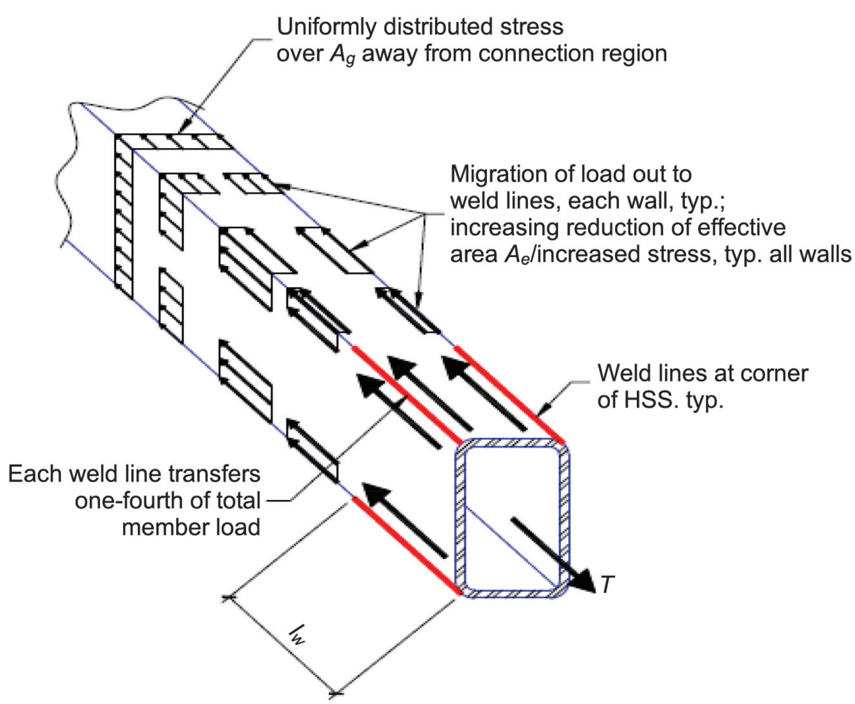

Fig. 1. In-plane shear lag in rectangular HSS connected with two side gusset plates with longitudinal welds.

Table 3. Parametric Study Matrix		
Configuration	**Perpendicular Distance between Welds**	**Length of Weld**
Gusset plates on H side	H	Varied from 0.25H up to 2H with an increment of 0.25H
Gusset plates on B side	B	Varied from 0.25B up to 2B with an increment of 0.25B
Gusset plates on H side	H	Varied from $0.25\left(\frac{H+B}{2}\right)$ up to $2\left(\frac{H+B}{2}\right)$ with an increment of $0.25\left(\frac{H+B}{2}\right)$
Gusset plate on B side	B	Varied from $0.25\left(\frac{H+B}{2}\right)$ up to $2\left(\frac{H+B}{2}\right)$ with an increment of $0.25\left(\frac{H+B}{2}\right)$

Combining the effects of both walls gives a total shear lag factor as given in Equation 6:

$$U_M = \frac{BU_B + HU_H}{B+H} \tag{6}$$

Equation 6 can then be used for rectangular and square HSS as follows

- Rectangular HSS

$$U_H = \frac{3l^2}{3l^2 + H^2} \tag{7}$$

$$U_B = \frac{3l^2}{3l^2 + B^2} \tag{8}$$

$$U_M = \frac{BU_B + HU_H}{B+H} \tag{9}$$

- Square HSS

$$H = B,\ U_H = U_B \tag{10}$$

$$U_M = \frac{3l^2}{3l^2 + B^2} \tag{11}$$

Parametric Study

A parametric study was performed based on the proposed equations for rectangular and square HSS sections; equations 9 and 11, respectively, for AISC *Specification* Case 6b. A total of 76 HSS sections were evaluated, where the thickest walls were randomly selected from each HSS family. For each specimen, a configuration of gusset plates on the H side and B side and weld lengths varying from 0.25H up to 2H, with an increment size of 0.25H, was considered. Various such configurations were considered as illustrated in Table 3. A comparison of the shear lag factors calculated based on current AISC *Specification* Case 6b and the new equation is presented. Bar charts are plotted to compare the shear lag factors calculated from the two methods. Comparisons for HSS 12×10×½ (H×B×t) and HSS 20×4×½ (H×B×t) are provided in Figures 2 and 3, respectively. Refer to the trends observed in the following section for discussion of the ratios shown above the bars in Figures 2 and 3. Note that

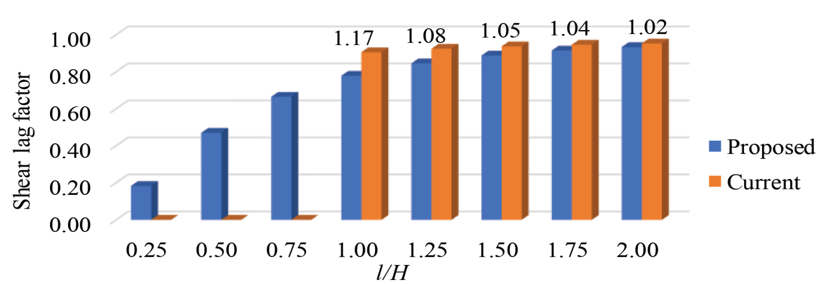

Fig. 2. Comparison of shear lag factor for the proposed equation with the current AISC Specification *Case 6b for* HSS 12×10×½ *(gusset plate on H side).*

the are no bars for the l/H and l/B less than 1, and no ratios are provided because the current AISC *Specification* Case 6b does not permit connections with l/H and l/B less than 1.

Parametric Study

- For HSS sections that are almost square or square—for example, a HSS 12×10×½—when the l/B ratio is greater than 1, the difference in the shear lag factor calculated from the current AISC *Specification* Case 6b procedure compared to the new proposed equation is negligible as seen in Figure 2 for the currently permitted cases where the weld length is at least as long as the width of the H dimension. However, the shear lag factor calculated from the proposed mathematical model is conservative when l/B ratio is equal to 1.
- Referring to Figure 2, another observation can be made that as the weld length is increased, the ratio of $U_{current}/U_{proposed}$ continually decreases from 1.17 to 1.02
- For gusset plates on the B side of the rectangular HSS member (refer to Figure 3), the shear lag factor calculated using the proposed model is higher as compared to the current Case 6b. This was observed when the l/B ratio is 1.25 and 1.5. When the ratio is 1.75 and 2.00, the proposed model predicts a smaller factor relative to the current AISC model.
- When using the current AISC model, HSS sections with high H/B ratios can result in negative shear lag values (i.e., when $l < \bar{x}$). This can be observed in Figure 3 for the HSS 20×4×½ with l/B equal to 1.00. In this case, the shear lag factor calculated using the proposed model is 0.27 and, from current Case 6b, is negative 0.04 (represented as zero in Figure 3). When l/B = 1.25, the proposed model predicts a value higher than the current Case 6b with the $U_{current}/U_{proposed}$ ratio being 0.63.
- For square HSS sections when l/B is 1.0, the ratio of $U_{current}/U_{proposed}$ is 1.17, and it continuously decreases to a final value of 1.02 when the l/B ratio is increased to 1.25, 1.5, up to 2, as seen in Figure 4.
- In general, it can be concluded that the shear lag factors calculated using the new proposed equations are slightly conservative as compared to current AISC *Specification* Case 6b except for the cases when H/B ratio is quite high. The proposed model also provides a non-zero shear lag factor for all cases and will not produce a negative value.

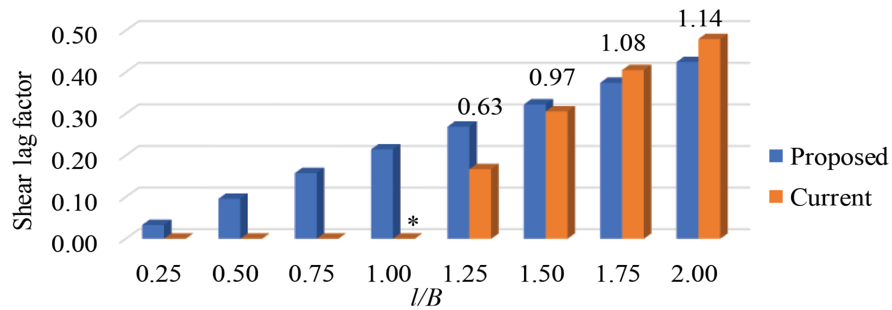

* *For l/B =1.00, U is negative using the current AISC* Specification *Case 6b.*

Fig. 3. Comparison of shear lag factor from the proposed equation with the current AISC Specification *Case 6b for* HSS 20×4×½ *(gusset plate on B side).*

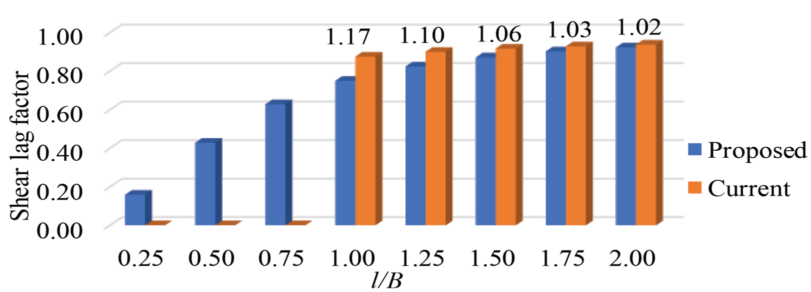

Fig. 4. Comparison of shear lag factor from the proposed equation with the current AISC Specification *Case 6b for* HSS 12×12×⅝ *(gusset plate on B).*

- The new proposed model permits weld lengths less than the perpendicular distance between the welds whereas the current procedure does not permit this.

FINITE ELEMENT ANALYSIS

The ABAQUS software package, using "explicit" analysis, was selected to perform the finite element analysis (FEA). A total of 31 members were modeled and evaluated in ABAQUS. The HSS members were modeled with square corners in lieu of rounded corners, and fillet welds were used in place of flare bevel groove welds, which would typically be required for the rounded corners of an HSS. One model was developed using rounded corners and flare bevel groove welds, and it was determined that the analysis is not sensitive to this particular detail. As such, for simplicity, square corners with fillets welds were used for this study. The preprocessing of the model was done in ABAQUS/CAE, and the ABAQUS dynamic explicit solver was selected to run all of the finite element analyses. The explicit procedure performs a large number of small time increments efficiently. It uses a form of the central difference time integration method to satisfy the dynamic equilibrium equations.

Material Properties

The modulus of elasticity was taken as 29,000 ksi, and Poisson's ratio was taken as 0.30 in accordance with industry standards. The material for the gusset plate was defined as elastic perfectly plastic with a yield stress of 50 ksi. A similar material type was defined for the weld material with an ultimate stress of 70 ksi. The stress strain curve for ASTM A500 Grade B, as shown in Figure 5, was used for the HSS steel material and was scaled to R_yF_y and R_tF_u to account for expected yield and tensile strengths, respectively.

The "ductile damage initiation criterion" was assigned to the HSS material. The ductile damage criterion deals with predicting the initiation of damage due to growth of voids and nucleation and provides a relationship among fracture strain, stress triaxiality, and strain rate. A reasonable value of 0.1995 was used for the fracture strain based on the stress strain curve used for the HSS material. When dynamic explicit analysis is performed, it is required to provide proper definition of density for all the materials. The density of the materials was taken as 0.1 kip/in^3 as recommended by Utsab Dhungana (2014). Table 4 shows the dimensions of the specimens as modeled in ABAQUS. At the connections, the weld lengths considered were 0.5H, 1.0H, 2.0H, and 1.0B, where H is the longer side of the HSS member. The parameters shown in Table 4 are calculated using the following equations:

Length of HSS section,

$$L_H = l + 4H + 20 \tag{12}$$

Length of gusset plate,

$$L_G = l + 2\frac{D}{16} \tag{13}$$

Width of gusset plate,

$$W = H + 2\tan(30)l \tag{14}$$

Thickness of the gusset plate,

$$T_G = \frac{\text{Applied load}}{F_y W} \tag{15}$$

Size of weld,

$$D = \frac{0.75(\text{Applied load})}{1.392ln} \tag{16}$$

Expected ultimate tensile capacity of the HSS section

$$= R_t F_u A_g \tag{17}$$

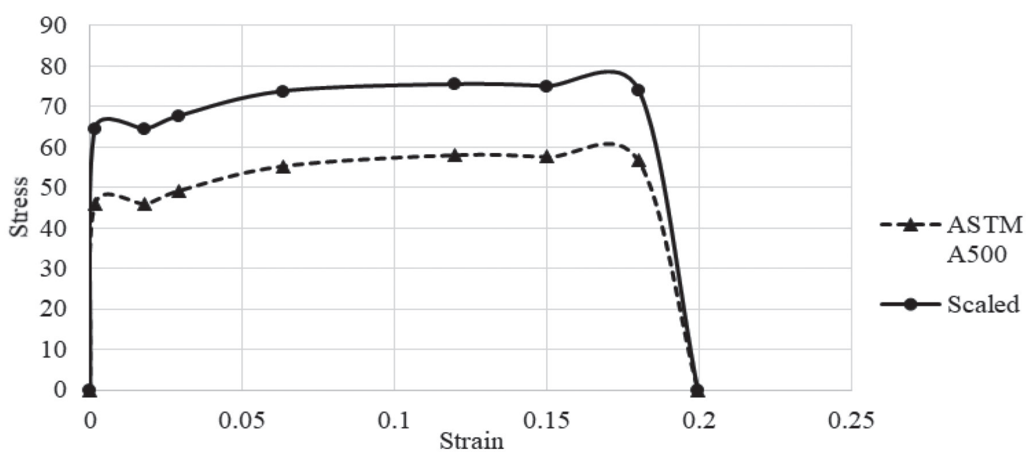

Fig. 5. Stress-strain curve for ASTM A500 Grade B.

Table 4. Model Details								
	HSS Section Details			Gusset Plate Details			Weld Details	
ID	Member	L_H (in.)	$R_t F_u A_g$ (kips)	L_G (in.)	W (in.)	T_G (in.)	D (16th of an inch)	l (in.)
1a*	4×4×½	38	528	6.50	11.3	0.50	36	2.0
1b		40		6.25	9.00	0.60	18	4.0
1c		44		9.13	13.5	0.40	9.0	8.0
2a*	6×6×⅝	47	1015	8.75	17.5	0.60	46	3.0
2b		50		8.88	13.0	0.80	23	6.0
2c		56		13.5	20.0	0.51	12	12
3a	8×8×⅝	56	1390	9.88	19.8	0.75	47	4.0
3b		60		11.0	17.0	0.80	24	8.0
3c		58		17.5	26.5	0.55	12	16
4a	12×6×⅝	74	1580	10.5	21.0	0.80	36	6.0
4b		80		14.3	26.0	0.65	18	12
4c		92		21.1	40.0	0.40	9.0	24
4d		50		10.5	15.0	1.10	36	6.0
5a	12×12×⅝	74	2140	12.1	24.3	0.90	49	6.0
5b		80		15.1	26.0	0.85	25	12
5c		92		25.6	40.0	0.55	13	24
6a	16×4×⅝	92	1770	11.8	26.0	0.70	30	8.0
6b		100		17.9	35.0	0.51	15	16
6c		116		33.0	53.0	0.35	8.0	32
6d		40		11.5	19.0	1.00	60	4.0
7a	16×16×⅝	92	2900	14.1	28.3	1.10	49	8.0
7b		100		19.1	34.5	0.85	25	16
7c		116		33.6	53.0	0.55	13	32
8a	20×4×½	110	1730	13.0	32.0	0.55	24	10
8b		120		21.5	23.0	0.40	12	20
8c		140		40.8	66.2	0.27	6.0	40
8d		40		9.88	15.8	1.20	47	4.0
9a	20×12×⅝	110	2900	15.0	31.6	0.95	40	10
9b		120		22.5	43.1	1.00	20	20
9c		140		41.3	66.2	0.45	10	40
9d		80		16.1	26	1.15	33	12

* Specimens were not used because the required weld sizes exceeded the width of the HSS wall.

For specimen 1a, the weld size required to transfer the expected tensile capacity of the HSS section was calculated to be 2.25 in. Two such welds would be required on each wall for the desired geometry of the analytical specimen, resulting in a dimension of 4.5 in., which is greater than the width of the HSS. A similar comment can be made for specimen 2a. Although a calculation can be made for the shear lag using the mathematical model, for the reasons previously mentioned, specimens 1a and 2a were not able to be modeled in ABAQUS.

The interaction of welds with the gusset plates and the HSS member was defined using tie constraints; tie constraints are found to be effective for welded connections (Ruffley, 2010). A fixed boundary condition was applied to the gusset plates attached to one end of the HSS member, and load was applied on the gusset plates attached to the other end of the HSS using kinematic coupling interactions. Figure 6 shows the assembly configuration, partitioning of the members, kinematic coupling interactions, and the welds attached to the gusset plate and HSS member via tie constraints for specimen HSS 12×12×⅝.

RESULTS AND DISCUSSION

All of the HSS specimens fractured at a section outside of the connection region. It was observed that the section fractured at a load smaller than the calculated expected tensile capacity of the section. All of the specimens yielded, and necking was clearly visible, followed by complete rupture of the HSS section. The reactions were taken at the gusset plate at the fixed boundary end of the specimen. The maximum value of the reaction at the fixed end is taken as the fracture load. The shear lag coefficient, U_F, was calculated as the ratio of this reaction force to the calculated expected tensile capacity $R_tF_uA_g$ of the HSS section. The FEA results for all the specimens are provided in Table 5.

The development of stresses in specimen 5b is shown in Figures 7(a), (b), (c), and (d). Figure 7(a) shows the specimen when there is zero load. Figure 7(b) shows the stress distribution when 85% of the applied load is transferred by the HSS section to the fixed end. At section *b-b* in Figure 7(b), it can be observed that there is a uniform distribution of stresses, whereas away from section *b-b* and closer to the connection region, there is nonuniform stress distribution. Similar stress distribution patterns were observed on each wall because of symmetry. In Figure 7(c) at section *c-c*, necking was observed, and the load transferred by the HSS section at that time was 86% of the applied load. Figure 7(d) shows fracture initiation at section *d-d* when the load transferred by the HSS section is equal to 87% of the applied load. Figure 8 shows an axonometric view of specimen 5b after fracture.

Table 6 shows a comparison between shear lag factors calculated from the three methods: AISC *Specification* Case 6b (U_A), mathematical model (U_M), and FEA (U_F).

Using the values provided in Table 6, graphs were generated, as shown in Figure 9, to compare the values of the shear lag factor from the three methods. Figure 9 compares the shear lag values for HSS 16×4×⅝ (specimen 6). It can be observed that when l/H is less than 1.0, current AISC *Specification* Case 6b does not permit such a connection, but the mathematical model gives a value of $U_M = 0.53$, which is conservative compared to the value obtained from FEA ($U_F = 0.76$). When l/H is 2.0, using the current AISC *Specification* Case 6b, the HSS section is 99% effective to carry or transfer load thus giving a shear lag factor of $U_A = 0.99$. However, the mathematical model and the FEA predict a shear lag value of $U_M = U_F = 0.94$.

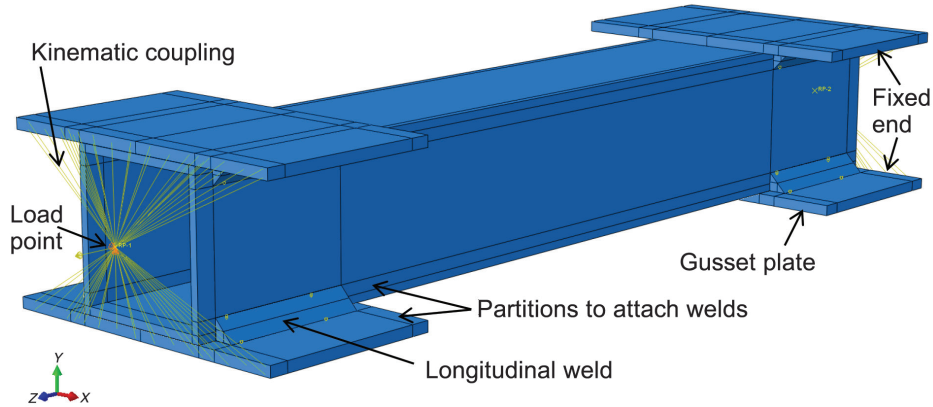

Fig. 6. Assembly configuration for HSS 12×12×⅝.

Table 5. FEA Results						
HSS Section Details			Weld Configuration		Failure Load (kips)	Shear Lag Factor, U_F
Specimen Designation	Member	$R_t F_u A_g$ (kips)	l (in.)			
1a	4×4×½	528	0.5H	2.0	NA	NA
1b			1.0H	4.0	485	0.92
1c			2.0H	8.0	460	0.87
2a	6×6×⅝	1010	0.5H	3.0	NA	NA
2b			1.0H	6.0	866	0.85
2c			2.0H	12	965	0.95
3a	8×8×⅝	1390	0.5H	4.0	1160	0.83
3b			1.0H	8.0	1190	0.86
3c			2.0H	16	1310	0.94
4a	12×6×⅝	1580	0.5H	6.0	1350	0.85
4b			1.0H	12	1370	0.86
4c			2.0H	24	1470	0.93
4d			1.0B	6.0	1480	0.94
5a	12×12×⅝	2140	0.5H	6.0	1670	0.78
5b			1.0H	12	1870	0.87
5c			2.0H	24	2010	0.94
6a	16×4×⅝	1770	0.5H	8.0	1340	0.76
6b			1.0H	16	1510	0.85
6c			2.0H	32	1660	0.94
6d			1.0B	4.0	1330	0.75
7a	16×16×⅝	2900	0.5H	8.0	2080	0.72
7b			1.0H	16	2480	0.86
7c			2.0H	32	2730	0.94
8a	20×4×½	1730	0.5H	10	1160	0.67
8b			1.0H	20	1619	0.93
8c			2.0H	40	1590	0.92
8d			1.0B	4.0	949	0.55
9a	20×12×⅝	2900	0.5H	10	2290	0.79
9b			1.0H	20	2650	0.91
9c			2.0H	40	2680	0.92
9d			1.0B	12	2440	0.84

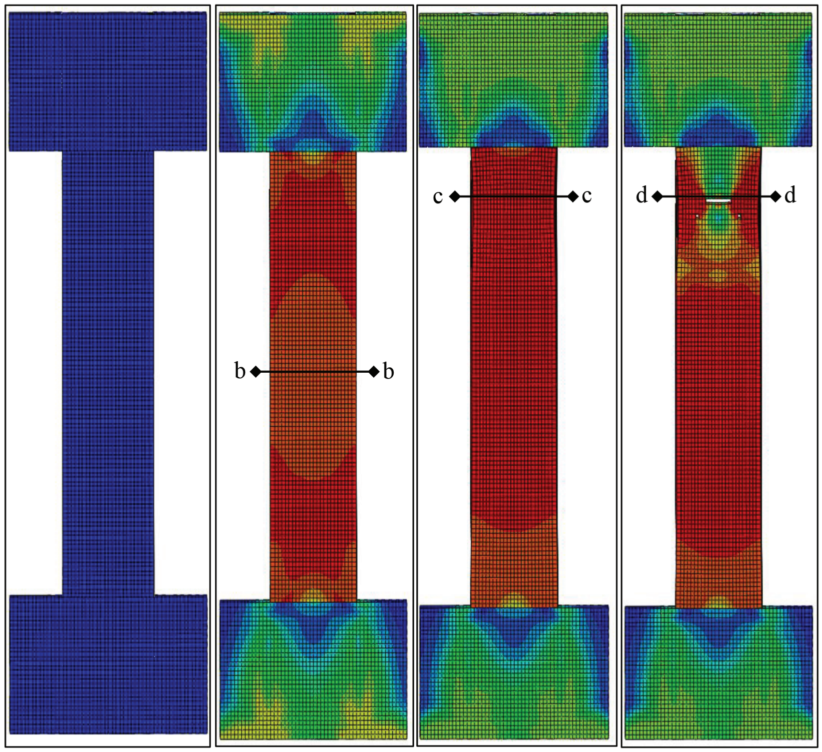

(a) Unloaded (necking) (b) 85% load (c) 86% load (fracture) (d) 87% load

Fig. 7. Development of stresses and fracture initiation in specimen 5b.

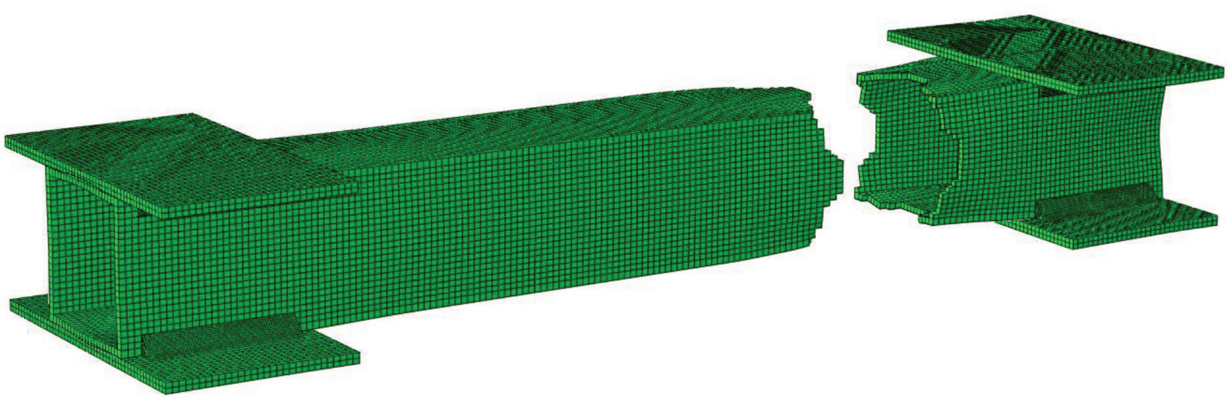

Fig. 8. Axonometric view of specimen 5b after fracture.

Table 6. Shear Lag Factors Comparison				
HSS Section Details		AISC *Specification*	Mathematical Model	FEA
Specimen Designation	Section	U_A^*	U_M	U_F
1a	4×4×½	NA	0.43	NA
1b		0.88	0.75	0.92
1c		0.94	0.92	0.87
2a	6×6×⅝	NA	0.16	NA
2b		0.88	0.75	0.85
2c		0.94	0.92	0.95
3a	8×8×⅝	NA	0.43	0.83
3b		0.88	0.75	0.86
3c		0.94	0.92	0.94
4a	12×6×⅝	NA	0.54	0.85
4b		0.96	0.81	0.86
4c		0.98	0.94	0.93
4d		0.67	0.54	0.94
5a	12×12×⅝	NA	0.43	0.78
5b		0.875	0.75	0.87
5c		0.94	0.92	0.94
6a	16×4×⅝	NA	0.53	0.76
6b		0.99	0.8	0.85
6c		0.99	0.94	0.94
6d		0.2	0.28	0.75
7a	16×16×⅝	NA	0.43	0.72
7b		0.88	0.75	0.86
7c		0.94	0.92	0.94
8a	20×4×½	NA	0.52	0.67
8b		0.99	0.79	0.93
8c		0.99	0.93	0.92
8d		NA	0.21	0.55
9a	20×12×⅝	NA	0.52	0.79
9b		0.94	0.8	0.91
9c		0.97	0.94	0.92
9d		0.74	0.61	0.84

* N/A denotes cases not currently permitted in AISC *Specification* for weld lengths less than *H* or *B*.

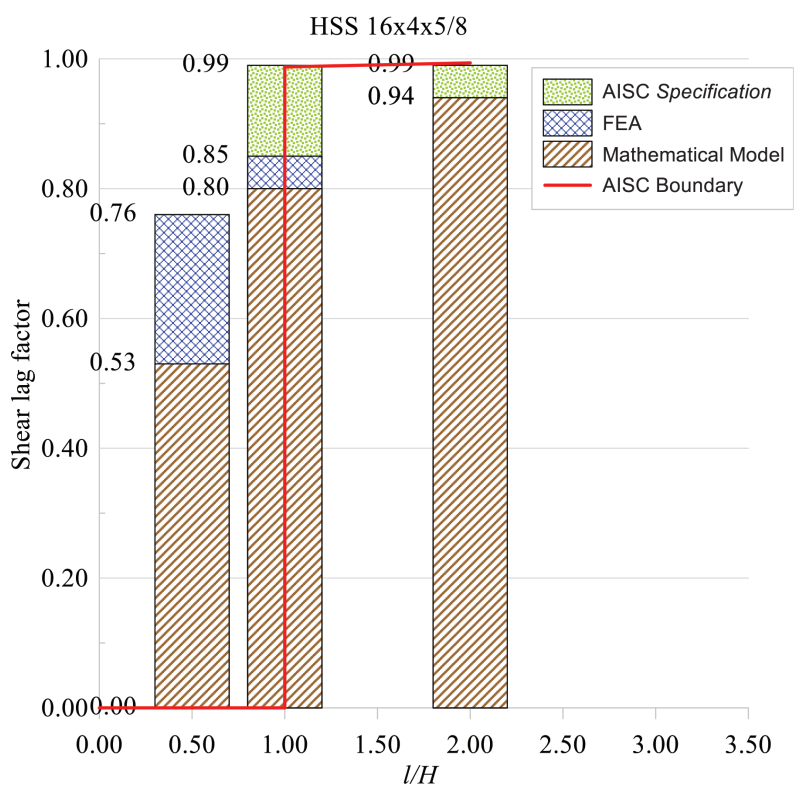

Fig. 9. Shear lag factor comparison.

CONCLUSIONS

Based on the presented results, the following can be concluded.

1. From the parametric study, the proposed mathematical model is conservative as compared to the current AISC *Specification* Table D3.1, Case 6b, except for some cases when the gusset plate is attached on the *B* side of the HSS.
2. The proposed model allows for weld lengths less than the distance between the welds.
3. The stress distribution pattern on which the mathematical model is based has good correlation with the FEA results.
4. The results from the finite element analyses are consistent with the values of the shear lag factors calculated using the proposed mathematical model.

RECOMMENDATIONS

1. It is recommended that AISC adopt the mathematical model proposed here and revise Case 6b of Table D3.1 of the AISC *Specification*.
2. Experimental testing should be performed to validate the results of the finite element analysis and provide more insights on some of the conclusions mentioned earlier.
3. The FEA models can be further refined by using actual material properties, measured from coupon tests, for the HSS ASTM A500 Grade B material.

SYMBOLS

A_g Gross area of the HSS section, in.^{2}

B Shorter side of the HSS section, in.

D Weld size in sixteenths of an in.

F_y Yield stress, ksi

F_u Ultimate tensile stress of the HSS section, ksi

H Longer side of the HSS section, in.

L_H Length of the HSS section, in.

L_G Length of the gusset plate, in.

P_B Tension load carried by *B* wall, kips

P_H Tension load carried by *H* wall, kips

P_u Total tension load, kips

R_t Correction factor

T_G Thickness of the gusset plate, in.

U Shear lag factor

U_A Shear lag factor calculated using the current AISC Case 6b

U_B Shear lag factor for *B* walls

$U_{Current}$ Shear lag factor calculated using the current AISC Case 6b

U_F Shear lag factor obtained from the finite element analysis

U_H Shear lag factor for *H* walls

U_M Shear lag factor calculated using the mathematical model

$U_{Proposed}$ Shear lag factor calculated using the proposed mathematical model

W Width of the gusset plate, in.

l Length of the weld, in.

n Number of welds

$\bar{x}$ Connection eccentricity, in.

w Width of the HSS, in.

REFERENCES

ABAQUS (2013), *Abaqus Analysis User's Manual,* Version 6.10, Simulia, Providence, R.I.

AISC (2010), *Specification for Structural Steel Buildings*, ANSI/AISC 360-10, American Institute of Steel Construction, Chicago, Ill.

AISC (2016), *Specification for Structural Steel Buildings*, ANSI/AISC 360-16, American Institute of Steel Construction, Chicago, Ill.

Dhungana, U. (2014), "Shear Lag Factor for Longitudinally Welded Tension Members Using Finite Element Method," MS Thesis, School of Civil and Environmental Engineering, University of Cincinnati, Ohio.

Fortney, P.J., and Thornton, W.A. (2012), "Recommendations for Shear Lag Factors for Longitudinally Welded Tension Members," *Engineering Journal*, AISC, Vol. 49, No. 1.

Ruffley, D.J. (2010), "A Finite Element Approach for Modeling Bolted Top-and-Seat Angle Components and Moment Connections," MS Thesis, School of Civil and Environmental Engineering, University of Cincinnati, Ohio.